



Universiteit
Leiden
The Netherlands

Liposome-based vaccines for immune modulation: from antigen selection to nanoparticle design

Lozano Vigario, F.

Citation

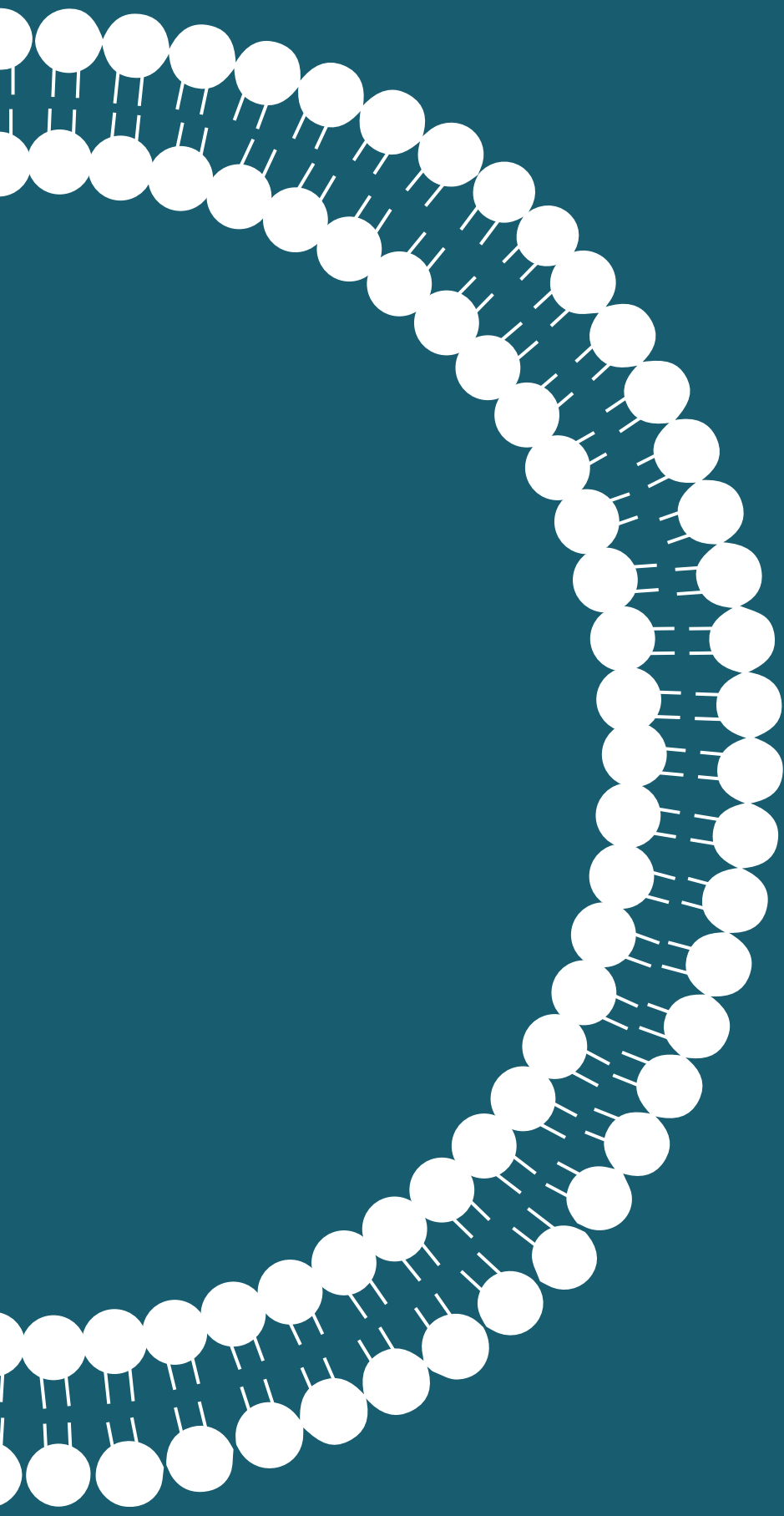
Lozano Vigario, F. (2024, September 10). *Liposome-based vaccines for immune modulation: from antigen selection to nanoparticle design*. Retrieved from <https://hdl.handle.net/1887/4082551>

Version: Publisher's Version

License: [Licence agreement concerning inclusion of doctoral thesis in the Institutional Repository of the University of Leiden](#)

Downloaded from: <https://hdl.handle.net/1887/4082551>

Note: To cite this publication please use the final published version (if applicable).



Chapter 6

Surface composition of nanoparticles rather than its rigidity, affects tolerogenic behaviour *in vivo*

F. Lozano Vigario¹, M.A. Neustrup¹, L. H. M. Burgmeijer¹, W.E. van der Heijden¹, A. Kros², J.A. Bouwstra¹, B.A. Slütter¹

¹ Division of BioTherapeutics, Leiden Academic Centre for Drug Research, Leiden University, The Netherlands

² Supramolecular & Biomaterials Chemistry, Leiden Institute of Chemistry, Leiden University, The Netherlands

ABSTRACT

The induction of antigen-specific immune tolerance using nanoparticles is a promising therapeutic strategy to arrest pathogenic immune responses in atherosclerosis. Previous research has shown that anionic liposomes containing 1,2-Distearoyl-sn-glycero-3-phosphoglycerol (DSPG) have intrinsic capacity to induce tolerogenic immune responses in mice. The tolerogenic properties of these liposomes has been associated to their high rigidity since saturated phospholipids form tightly packed lipid bilayers and rigid liposomes. However, the phospholipid composition can also determine the protein corona formed around the nanoparticles when in a biological fluid. Here, we made use of DOPG/PLGA hybrid nanoparticles with a poly(lactic-co-glycolic acid) (PLGA) core, that provides rigidity, surrounded by loosely packed DOPC:DOPG lipid bilayer to determine the contribution of nanoparticle rigidity to tolerogenic immune responses *in vitro* and *in vivo*. We show that although the DOPG/PLGA hybrid nanoparticles are able to deliver the antigen to dendritic cells and induce antigen-specific T cell responses *in vitro*, they fail to replicate the same effect *in vivo*. We hypothesize that these differences might be due to the different protein coronas formed around the particles and that, at least *in vivo*, the protein corona might play a bigger role than the nanoparticle rigidity in the efficacy of lipid-based formulations. We show that while the uptake of DSPG liposomes is mediated by C1q, the uptake of the DOPG/PLGA hybrid nanoparticles might be mediated by ApoB100. In conclusion, our data suggests that the lipid bilayer composition and the set of proteins attracted to the nanoparticle surface might be more important than the particle rigidity to determine their *in vivo* behaviour.

INTRODUCTION

Nanoparticles can be used for the delivery of antigens to antigen presenting cells (APCs), such as dendritic cells. The use of liposomes and other lipid-based nanoparticles for the induction of immune tolerance has been explored in previous studies and it is a promising novel therapeutic approach to treat inflammatory and autoimmune diseases^{1, 2}. Atherosclerosis is an example of such a disease, where the inflammatory response accelerates the growth of atherosclerotic plaques that eventually leads to cardiovascular events³.

The physicochemical characteristics of nanoparticles are key for their capacity to induce tolerogenic responses⁴. For example, liposome formulations with anionic ζ -potential have shown to have better capacity to induce T regulatory cells (Tregs)¹, the main mediators of peripheral tolerance, while cationic nanoparticles stir the immune response towards a pro-inflammatory T helper 1 or cytotoxic CD8⁺ T cell response⁵. Furthermore, the liposomal rigidity has also shown to be important in the tolerogenic capacity of liposomal formulations⁶. Previous work in our group has shown that the rigidity of liposomes measured by atomic force microscopy correlates with their capacity to induce Tregs⁶ and that highly rigid anionic liposomes containing the saturated anionic phospholipid 1,2-distearoyl-sn-glycero-3-phospho-(1'-rac-glycerol) (DSPG) are able to induce Tregs and to attenuate the development of atherosclerosis in mice¹. The tolerogenic capacity of these formulations has also been studied in both *in vitro* and *ex vivo* human models⁷.

The main determinant of liposome rigidity is the phospholipid composition, more specifically the level of saturation in the acyl chains of phospholipids and the presence of cholesterol in the bilayer⁸. The presence of saturated acyl chains will lead to more tightly packed bilayers and therefore higher particle rigidity⁹. However, the phospholipid organization in the bilayer and the presence of cholesterol can also alter the protein corona of the nanoparticles¹⁰. Therefore, when studying the relationship between nanoparticle rigidity and their immune modulating properties, the different lipid composition can be a confounding factor.

Here, we make use of DOPG/PLGA hybrid nanoparticles to determine the contribution of nanoparticle rigidity to tolerogenic immune responses *in vitro* and *in vivo*. These hybrid nanoparticles will have a high rigidity due to the solid PLGA polymeric core, but they also have the surface characteristics of a loosely packed lipid bilayer. We therefore compare the tolerogenic capacity of three different lipid-based formulations with different rigidity. One formulation consisting of the unsaturated phospholipids 1,2-dioleoyl-sn-glycero-3-phosphocholine (DOPC) and 1,2-dioleoyl-sn-glycero-3-phospho-(1'-rac-glycerol) (DOPG) (Figure 1A), forming more disordered and fluid liposome bilayer at physiological temperature

(37°C). Another formulation containing the saturated phospholipids 1,2-distearoyl-sn-glycero-3-phosphocholine (DSPC), 1,2-distearoyl-sn-glycero-3-phospho-(1'-rac-glycerol) (DSPG) and cholesterol (Figure 1B) forming a more ordered and tightly packed liposome bilayer and therefore more rigid. The presence of unsaturated vs saturated phospholipids in these two formulations makes the rigidity of these liposomes very different⁶. The DOPG/PLGA hybrid nanoparticle formulation (Figure 1C) consists of a poly(lactic-co-glycolic acid) (PLGA) polymeric nanoparticle surrounded by DOPC:DOPG lipid bilayer. To follow the antigen-specific immune response to these formulations, we loaded the particles with the model antigen OVA₃₂₃₋₃₃₉ (OVA323), that can be recognized by CD4⁺ T cells isolated from OT-II transgenic mice. Previous research has shown that the inclusion of the tolerogenic adjuvant 1 α ,25-Dihydroxyvitamin D3 (vitaminD3) is key for the translation of these tolerogenic formulations from pre-clinical research to the patients⁷, therefore all formulations studied here included vitaminD3.

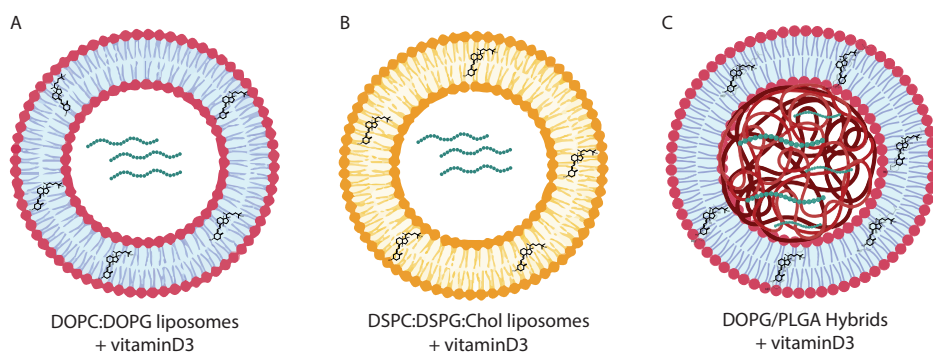


Figure 1. Schematic representation of nanoparticle formulations compared in this study. (A) Less rigid DOPC:DOPG liposome formulation with vitaminD3 in the lipid bilayer and OVA323-339 in the aqueous core. (B) Highly rigid DSPC:DSPG:Cholesterol liposomes with vitaminD3 and OVA323-339. (C) DOPG/PLGA hybrid nanoparticle with vitaminD3 in lipid bilayer and OVA323-339 in PLGA core.

MATERIAL AND METHODS

Materials

Phospholipids DOPC, DOPG, DSPC, DSPG and 1,2-dipalmitoyl-sn-glycero-3-phosphoethanolamine-N-(lissamine rhodamine B sulfonyl) (Liss-Rho-DPPE) were purchased from Avanti Polar Lipids (Birmingham, AL, USA). Cholesterol and poly(D,L-lactide-co-glycolide) (PLGA) were purchased from Sigma-Aldrich. T116-203 Interconnect Tee junctions were obtained from Mengel Engineering (Virum, Denmark). Staggered herringbone micromixer was purchased from Darwin

Microfluidics (Paris, France). Spectra-Por® Float-A-Lyzer were obtained from Sigma-Aldrich. 1 α ,25-Dihydroxyvitamin D3 (vitaminD3) was purchased from Sigma-Aldrich. OVA₃₂₃₋₃₃₉ (OVA323) was purchased from Invivogen (Toulouse, France). RPMI 1640 culture medium was obtained from Lonza (Basel, Switzerland). Fetal Bovine Serum (FBS) was purchased from Sigma-Aldrich (Zwijndrecht, Netherlands), penicillin/streptomycin from Fisher Scientific (Landsmeer, Netherlands) and L-glutamine was purchased from VWR (Amsterdam, Netherlands). CellTrace™ CFSE cell proliferation kit was obtained from ThermoFisher Scientific (MA, USA). Granulocytes-macrophages colony stimulating factor (GM-CSF) was purchased from ImmunoTools (Friesoythe, Germany). CD4 T cells isolation kit was obtained from Miltenyi Biotec (Leiden, the Netherlands). Anti-mouse CD3e (clone 145-2C11) and anti-mouse CD28 (clone 37.51) antibodies were purchased from Invitrogen (Waltham, Massachusetts, USA). *E. coli*-derived lipopolysaccharide (LPS) was purchased from Invivogen (Toulouse, France). Tissue-Tek® O.C.T. Compound was purchased from Sakura Finetek (CA, USA). 12-myristate 13-acetate (PMA) and ionomycin were purchased from Sigma Aldrich. BrefeldinA was obtained from ThermoFisher Scientific. Human C1q and human apolipoprotein B (ApoB) were purchased from Millipore (Merck, Darmstadt, Germany). Human apolipoprotein E (ApoE) was purchased from Sigma Aldrich (Zwijndrecht, Netherlands).

Animals

C57Bl/6, OT-II and ApoB100-OVA LDLR^{-/-} mice were bred in-house under standard laboratory conditions. ApoB100-OVA LDLR^{-/-} transgenic mice were generated in collaboration with the Department of Molecular Genetics and Translational Biology at University Medical Center Groningen. These mice were genetically modified using CRISPR/Cas9 technology to express a heterozygous genetic insertion of the two immunodominant epitopes of chicken ovalbumin, OVA₃₂₃₋₃₃₉ and OVA₂₅₇₋₂₆₄ in the C-terminal domain of ApoB100. All animals received water and food *ad libitum*. All experiments were approved by Animal Welfare Body of Leiden University and were performed in accordance with the Dutch government guidelines and Directive 2010/63/EU of the European Parliament.

Preparation of DOPG liposomes

DOPC:DOPG liposomes were prepared using a co-flow microfluidics system. Phospholipids DOPC and DOPG dissolved in ethanol absolute were mixed in a 4:1 molar ratio. Organic phase consisted on DOPC:DOPG lipid mix in ethanol at a concentration of 10 mg/mL. In formulations containing vitaminD3, this adjuvant was included in the organic phase. For fluorescently labelled formulations, 0.1 mol% of DOPC was substituted with Liss-Rho-DPPE. Aqueous phase consisted of PBS 1x containing OVA323 antigen. The organic and aqueous phases were combined in a

flow rate ratio of 2:1 using a T116-203 Interconnect Tee using NE300 syringe pumps (ProSense B.V., Oosterhout, The Netherlands) and Hamilton gastight glass syringes (Brunschwig Chemie B.V., Amsterdam, The Netherlands). The two phases passively mix in a 40 cm loop PEEK tube with an internal diameter of 0.5 mm. Formulations were dialyzed overnight against PBS 1x under constant stirring using Float-A-lyzer dialysis tube (MWCO 100,000Da) to remove organic solvent and non-encapsulated peptides and/or adjuvant.

Preparation of DSPG liposomes

DSPG:DSPG:CHOL liposomes were prepared as previously described¹¹. Briefly, DSPC, DSPG and cholesterol dissolved in ethanol absolute were combined in a 4:1:2 molar ratio at a total lipid concentration of 10 mg/mL. For the formulations containing vitaminD3, this was included in the organic phase together with the lipids. The aqueous phase consisted of phosphate buffer (PB) 10mM pH 7.4. For fluorescently labelled formulations, 0.1 mol% of DSPC was substituted with Liss-Rho-DPPE. The antigen OVA323 was included in the aqueous phase. The aqueous and organic phases were mixed using a staggered herringbone micromixer submerged in a water bath at 60°C. The two phases were mixed at a 2:1 (aqueous:organic) flow rate ratio and a total flow rate of 500 μ L/min. Formulations were dialyzed overnight using a Float-A-lyzed dialysis tube (MWCO 100,000 Da) under constant stirring against PB 10 mM pH 7.4.

Preparation of DOPG/PLGA hybrid nanoparticles

Hybrid nanoparticles were prepared using a custom-made three-syringe microfluidics system. Particles were prepared in two consecutive steps, in the first step PLGA dissolved in acetonitrile at 3 mg/mL was mixed with an aqueous phase consisting of either milliQ water or OVA323 dissolved in milliQ water. This initial mixing step was performed using a T116-203 Interconnect Tee. The output of this mixing step is PLGA particles that mix in another T116-203 Interconnect Tee with an organic phase consisting on DOPC:DOPG (4:1 molar ratio) at 3 mg/mL concentration in ethanol absolute. For fluorescently labelled formulations, 0.1 mol% of DOPC was substituted with Liss-Rho-DPPE. The flow rate ratio used was 3:1:1 (Aqueous:PLGA:lipids) and a total flow rate of 6250 μ L/min. Flow rate was controlled using NE300 syringe pumps and the aqueous, PLGA and lipid phases were loaded in Hamilton gastight glass syringes. After preparation, the organic solvent was partially evaporated for 30 minutes under an N₂ stream, and the formulations were dialyzed overnight using a Float-A-lyzed dialysis tube (MWCO 100,000Da) against milliQ water under constant stirring.

Characterization of formulations

Average hydrodynamic diameter (z-average) and polydispersity index (Pdl) of the formulations were determined using Dynamic Light Scattering (DLS) using a Zetasizer NanoZS (Malvern Panalytical, UK). The ζ -potential of the nanoparticles was determined by laser doppler electrophoresis using the same instrument.

Bone marrow derived dendritic cell culture

Immature dendritic cells were differentiated from pluripotent bone marrow cells isolated from femur and tibias of C57Bl/6 mice. Mice were sacrificed by cervical dislocation and femurs and tibias were collected. Bone marrow cells were extracted, and a single cell suspension was obtained by flushing the bone marrow out of the bones with PBS over a 70 μ m cell strainer. Cells were cultured for 10 days at 37°C and 5% CO₂ at a cell density of 2x10⁶ cells in 95 mm Petri dishes in complete RPMI (cRPMI). cRPMI consisted of RPMI supplemented with 10% v/v fetal bovine serum (FBS), 2 mM L-glutamine, 100 U/mL penicillin/streptomycin and 50 μ M β -mercaptoethanol. Furthermore, the medium was supplemented with 20 ng/mL granulocytes-macrophages colony stimulating factor (GM-CSF). Cell medium was refreshed every 2 days.

CD45.1 CD4 OT-II T cells isolation

OT-II transgenic mice were sacrificed by cervical dislocation and spleens collected. Spleens were strained through 70 mm cell strainer to obtain a single cell suspension. Red blood cells were lysed using ACK lysis buffer and CD4⁺ T cells were isolated using CD4 T cells isolation kit.

Effect of formulations on bone marrow-derived dendritic cells

Immature DCs were collected from 95 mm Petri dishes and 50,000 cells/well were seeded in U-bottom 96-well plates. Cells were exposed to the formulations for 4h, after which the formulations were removed from the wells and the DCs were thoroughly washed with PBS to remove the nanoparticles that were not taken up. Cells were incubated overnight with cRPMI medium supplemented with 20 ng/mL GM-CSF and 100 ng/mL *E. coli*-derived lipopolysaccharide (LPS). Cells were stained for MHC-II-eFluor450, CD11c-FITC, CD40-PE, CD86-APC and Fixable Viability Dye-APC-eFluor780 followed by flow cytometry analysis using a Cytotoflex flow cytometer (Beckman Coulter, CA, USA).

Effect of primed dendritic cells on T cell polarization

Immature DCs were cultured and exposed to formulations as described above. Cells were seeded in 96-well U-bottom plates at 25,000 cells/well and exposed to

the formulations for 4 hours. The dose of OVA323 was 1 nmol for those conditions receiving OVA-loaded particles or free OVA controls. Formulations were washed away, and cells were incubated overnight with 100 ng/mL LPS and 20 ng/mL GM-CSF in cRPMI medium. After overnight incubation, medium was removed and 100,000 CFSE-labelled OT-II CD4⁺ T cells per well were added. DCs and OT-II T cells were co-culture for 72 hours at 37°C and 5% CO₂. Cells were stained for Thy1.2-PE-Cy7, CD4-eFLuor450, FoxP3-PE, Tbet-APC, RORγT-Brilliant Violet 650 and Fixable Viability Dye-APC-eFLuor780.

Analysis of antigen-specific CD4⁺ T cell responses in vivo

Eight- to twelve-week-old mice were weighted and randomly allocated into groups of 5 mice. RandoMice® software (v1.1.1) was used for randomization and allocation of the mice to the experimental groups using weight as blocking factor¹². On day 0, all animals received an intravenous (IV) injection via tail vein of 500,000 OT-II CD4⁺ T cells. On day 1, animals received an IV injection in the tail vein of DOPC:DOPG liposomes, DSPC:DSPG:CHOL liposomes or DOPG/PLGA hybrid nanoparticles containing 1 nmol of OVA323 and 1-6.5 μg of vitaminD3. Empty DOPG/PLGA hybrid nanoparticles and 1 nmol free OVA323 and 6.5 μg vitaminD3 were used as control. On day 7, animals were sacrificed by cervical dislocation and spleens were collected. Single-cell suspension of the spleens was obtained by mashing them through a 70 μm cell strainer. Red blood cells were lysed using ACK lysis buffer, and the splenocytes were transfer to U-bottom 96-well plates for *ex vivo* re-stimulation and flow cytometry staining. Cells were stained for Thy1.2-AlexaFluor700, CD4-Brilliant Violet 510, CD45.1-eFLuor450, FoxP3-PE, Tbet-APC, RORγT-Brilliant Violet 650, CTLA4-Brilliant Violet 605, CD73-PE-Cy7, CD69-PE and Fixable Viability Dye-APC-eFLuor780. Stained cells were analysed by flow cytometry on a Cytoflex S (Beckman Coulter).

Effect of DOPG/PLGA hybrid nanoparticles in atherosclerosis

LDLr^{-/-} x ApoB100-OVA transgenic mice between 8 and 12 weeks old were weighted and randomly allocated to either treatment (n =15) or control group (n = 15) using RandoMice® software (v1.1.1) and weight as blocking factor for the randomization¹². At the start of the experiment animals are put on western-type diet consisting of 0.25% cholesterol and 15% cocoa butter (Special Diet Services, Essex, UK). On day 0, all animals received an IV injection of 1 x 10⁶ OT-II CD4⁺ T cells via the tail vein. Before adoptive transfer, OT-II CD4 T cells were activated by overnight incubation with 0.5 μg/ml antiCD3 and antiCD28 antibodies. On day 1, animals in the treatment group received an IV injection of DOPG/PLGA hybrid nanoparticles

loaded with 1 nmol OVA323 and 3.5-8 μg of vitaminD3, while animals in the control group received DOPG/PLGA hybrid nanoparticles with the same dose of vitaminD3 but no OVA323 antigen. Immunizations were repeated on days 22 and 43 of the experiment. Blood samples were collected 1 week after each immunization and animals were weighted weekly. On day 70, animals were weighted and anesthetized with an intraperitoneal injection of 10 mg/kg xylazine and 100 mg/kg ketamine. Anesthetized mice were exsanguinated and perfused by transcardiac perfusion using PBS. Spleen, aorta, hearts, and heart lymph nodes were collected. Spleens were processed as described above. Aortas were digested for 30 minutes at 37°C with collagenase I, collagenase XI, DNase and hyaluronidase. Single-cell suspensions of the aortas were obtained by passing the digested tissue through 70 μm cell strainer. Cells were transferred to U-bottom 96-well plates and stained for Thy1.2-Alexa Fluor 700, CD8a-Brilliant Violet 510, CD4-Brilliant Violet 650, CD45.1-eFluor450, CD45-FITC, CD11b-PE-Dazzle594, FoxP3-PE, Tbet-APC and Fixable Viability Dye-APC-eFluor780. Hearts were embedded and frozen in Tissue-Tek® O.C.T. Compound and 7 μm cryosections of the trivalve area were obtained using a Leica CM1950 (Leica Biosystems, Wetzlar, Germany). Sections were stained for Oil-Red-O (ORO) to visualize lipid-rich areas and Masson's trichrome staining to determine collagen content. Microscopy images of the stained slides were taken using Panoramic 250 Flash III slide scanner (3DHitech, Budapest, Hungary) and images were analysed using a custom-made macro in Fiji image processing software¹³.

Quantification of plasma cholesterol levels

Plasma was obtained by centrifugation of EDTA-treated blood at 2000 G for 10 minutes at 4°C and stored at -20°C until cholesterol quantification. Total cholesterol was determined using Roche/Hitachi enzymatic colorimetric assay and using Precipath standardized serum (Roche Diagnostics) as standard.

Effect of protein corona on particle size distribution and ζ -potential

Formulations were mixed at a lipid concentration of 0.5 mg/mL with 10% (v/v) mouse serum, 10% (v/v) FBS, 2 $\mu\text{g}/\text{mL}$ ApoE, 10 $\mu\text{g}/\text{mL}$ ApoB or 10 $\mu\text{g}/\text{mL}$ C1q. Protein concentrations used in this study are physiologically relevant and based on previous protein corona studies^{1, 14, 15}. Formulations at 0.5 mg/mL diluted in either PBS (DOPC:DOPG liposomes) or PB (DSPC:DSPG:Cholesterol liposomes and DOPG/PLGA hybrids) without protein were used as control. Formulations with or without protein were incubated for 1h at 37°C and unbound proteins were subsequently washed twice using a Vivaspin 500 centrifugal concentrator (MWCO 300 kDa, Sartorius, Göttingen, Germany). Z-average, Pdl and ζ -potential were determined

by DLS and laser doppler electrophoresis in a Zetasizer Ultra (Malvern Panalytical Ltd., UK).

Effect of protein corona on particle uptake by BMDCs

Bone marrow-derived dendritic cells (BMDCs) were seeded in a U-bottom 96-well plate at a concentration of 30,000 cells/well. DOPC:DOPG liposomes, DSPC:DSPG:Cholesterol liposomes or DOPG/PLGA hybrids labelled with Liss-Rho-DPPE were added to the wells at a lipid concentration of 20 $\mu\text{g}/\text{mL}$. The cell culture medium in the wells was either serum free (no protein control) or contained 10% mouse serum, 10% FBS, 2 $\mu\text{g}/\text{mL}$ ApoE, 10 $\mu\text{g}/\text{mL}$ ApoB or 10 $\mu\text{g}/\text{mL}$ C1q. BMDCs were exposed to formulations for 3.5h at 37°C and 5% CO₂, or at 4°C (control). Excess nanoparticles and proteins were removed by washing the cells twice with PBS and BMDCs were incubated overnight with cRPMI medium supplemented with 20 ng/mL GM-CSF at 37°C and 5% CO₂. Cells were subsequently stained with CD11c-FITC and Fixable Viability Dye-APC-eFluor780 for flow cytometry analysis. Stained cells were analysed on a Cytoflex S (Beckman Coulter).

Statistics

Statistical differences between groups were determined by one-way or two-way ANOVA followed by Tukey's or by Dunnett's multiple comparison test. P-values lower than 0.05 were considered statistically significant. Analysis was performed using GraphPad Prism for Windows (GraphPad Software, San Diego, California, USA).

RESULTS

Nanoparticle characterization

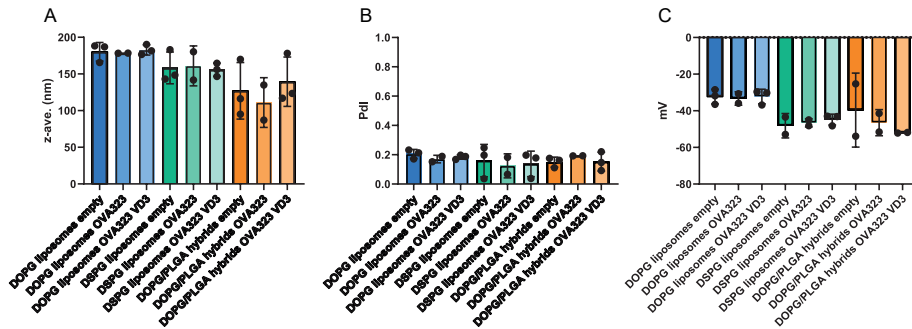


Figure 2. Characterization of nanoparticles by dynamic light scattering and laser Doppler electrophoresis. (A) Average hydrodynamic diameter of the nanoparticles (Z-average) in nm, (B) Polydispersity Index and (C) ζ -potential in mV of DOPG liposomes, DSPG liposomes and DOPG/PLGA hybrid nanoparticles either empty, loaded with the antigen OVA323 or both OVA323 and the adjuvant vitaminD3 (VD3). Data shown is mean \pm SD from at least two independent formulation batches ($n \geq 2$).

Nanoparticle size has an impact in the biological effect and biodistribution of the formulations, with a particle size between 100 and 200 nm being the most optimal for the induction of DCs-mediated antigen-specific immune responses⁴. All generated formulations have an average hydrodynamic diameter (z-ave.) within this size range, with DOPG/PLGA hybrid nanoparticles closer to 100 nm and the slightly larger DOPG liposomes around 180 nm (Figure 2A). Polydispersity index (Pdl) of the formulations is a quality attribute that indicates the width of the size distribution. All formulations have a Pdl around 0.2 or lower, indicating a monodisperse size distribution (Figure 2B). Finally, the ζ -potential of the formulations, a measurement of the surface charge of the nanoparticles, is between -25 mV and -55 mV (Figure 2C), indicating that all formulations are strongly negatively charged.

Anionic nanoparticles have a tolerogenic effect on dendritic cells in vitro

To assess the tolerogenic effect of the formulations on DCs, we cultured dendritic cells from murine bone marrow (BMDCs) and exposed them to the formulations. Tolerogenic DCs are characterized by the expression of lower levels of co-stimulatory molecules such as CD86 or CD40 upon pro-inflammatory stimulation, therefore maintaining an immature phenotype¹⁶. The immature DCs were exposed to DOPG liposomes, DSPG liposomes or DOPG/PLGA hybrid nanoparticles loaded with vitaminD3 for 4 hours. Subsequently, formulations were thoroughly

washed away, and cells were incubated overnight with 100 ng/mL of LPS. Next, the expression of CD86 and CD40 was measured by flow cytometry (Figure 3A). We observed a significant decrease in the percentage of DCs expressing both CD86 and CD40 (Figure 3B) in the DSPG liposomes and DOPG/PLGA hybrid nanoparticles conditions compared to the medium control with this reduction being more pronounced in the DOPG/PLGA hybrids condition. Furthermore, the geometric mean fluorescence intensity (gMFI) of CD86 was significantly reduced in all formulations compared to medium control but also to the free vitaminD3 control (Figure 3C), indicating that the formulation of vitaminD3 in liposomes boosts its tolerogenic potential. The expression of the co-stimulatory molecule CD40 was also lower in all formulations compared to medium control, but in this case the free vitaminD3 also affected CD40 expression (Figure 3D). Thus, on the DCs level, the most rigid DOPG/PLGA particles showed the most potent tolerogenic properties.

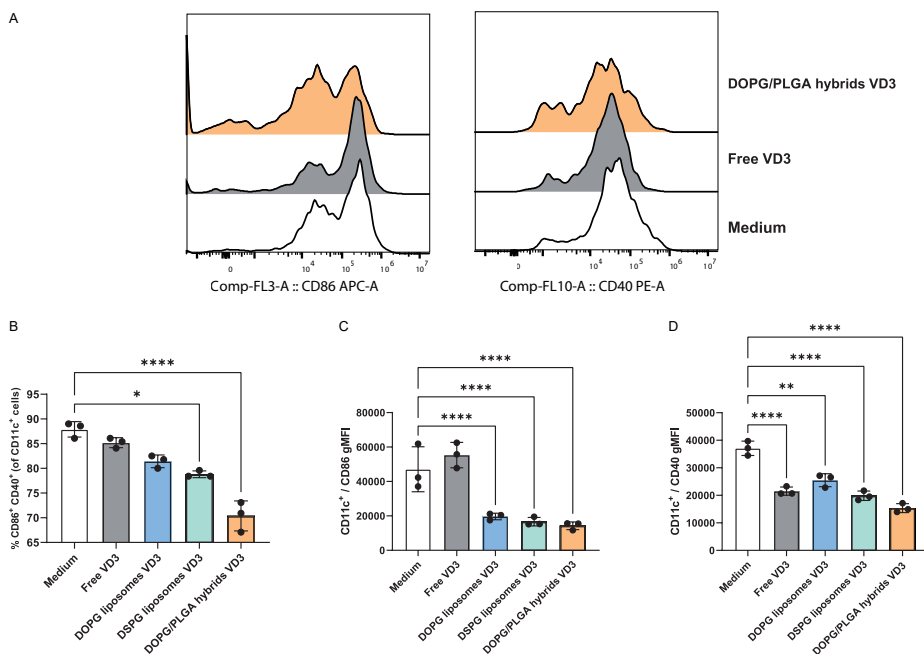


Figure 3. Effect of nanoparticle in expression of activation markers in BMDCs after pro-inflammatory stimulus. (A) Representative histograms of CD86 and CD40 expression in BMDCs treated with DOPG/PLGA hybrids loaded with VD3, free VD3 control or medium control. (B) Percentage of CD11c⁺ cells expressing both CD86 and CD40. (C) Geometric mean fluorescence intensity (gMFI) of antiCD86 within the CD11c⁺ population. (D) Geometric mean fluorescence intensity (gMFI) of antiCD40 within the CD11c⁺ population. **** $p \leq 0.0001$, *** $p \leq 0.001$, ** $p \leq 0.01$, * $p \leq 0.05$ determined by one-way ANOVA and Tukey's multiple comparison test.

DOPG/PLGA hybrid nanoparticles induce antigen-specific T cell proliferation and increase FoxP3, ROR γ T and Tbet expression compared to liposomes

Since the induction of immature DCs by the formulations suggests the initiation of tolerogenic responses, we next studied the effect of nanoparticle-primed DCs on T cell proliferation and polarization. For that, BMDCs were exposed to nanoparticles either empty, loaded with the model antigen OVA323 or loaded with OVA323 and vitaminD3. Primed DCs were co-culture for 72 hours with OVA323-specific CD4⁺ T cells isolated from the spleen of OT-II mice. All three nanoparticle formulations loaded with antigen were able to induce T cell proliferation to a level similar as the positive control, free OVA323 condition (Figures 4A, B). When looking further into the population of proliferating cells, we observed that only the DCs primed with OVA-loaded DOPG/PLGA hybrid nanoparticles were able to induce significant upregulation of the transcription factor FoxP3, which is the main driver of a Treg phenotype (Figure 4C). However, for the DOPG/PLGA hybrid nanoparticle conditions we also observed an increase in expression of transcription factors ROR γ T and Tbet (Figure 4D and 4E), associated to Th17 and Th1 cells respectively, which was suppressed by inclusion of vitaminD3. Interestingly, both DOPG liposomes and DSPG liposomes loaded with OVA323 and vitaminD3 led to a significant lower expression of the Th1-associated transcription factor Tbet compared to the free antigen control (Figure 4E), suggesting that although these particles did not trigger strong Treg responses, they did reduce the overall inflammatory phenotype of the CD4⁺ T cells.

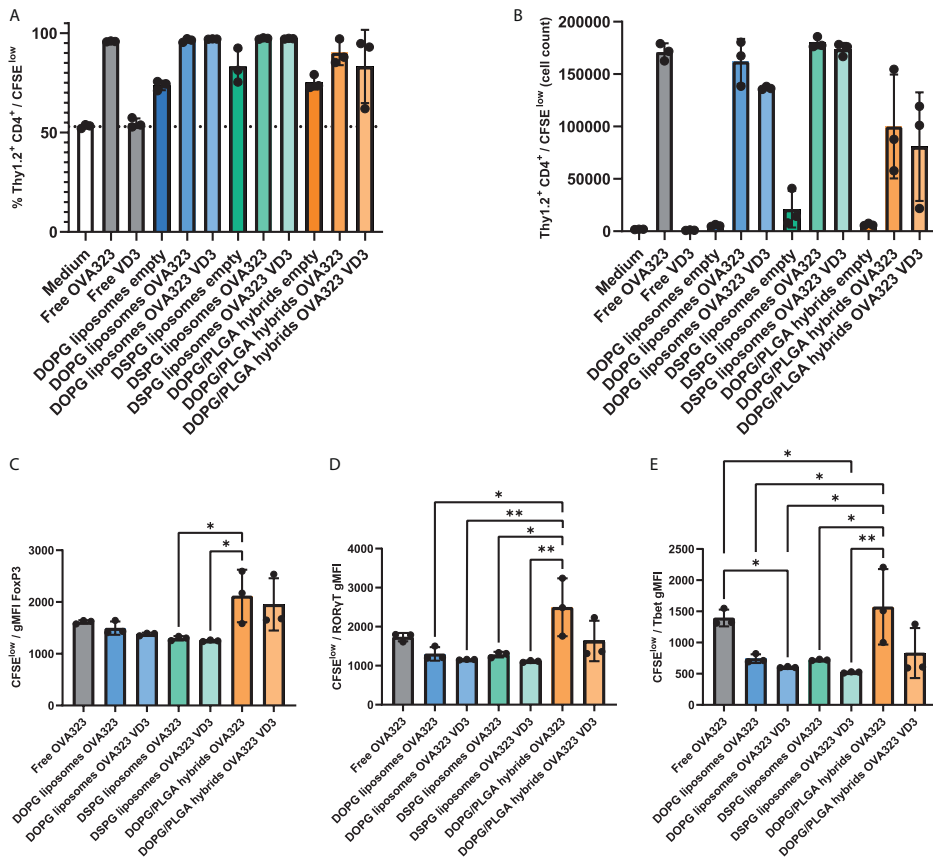


Figure 4. Effect of nanoparticle-primed BMDCs on T cells proliferation and differentiation in vitro. (A) Percentage of CD4⁺ T cells (Thy1.2⁺ CD4⁺) that proliferated (CFSE^{low}) during BMDC and T cell co-culture. (B) Number of proliferated CFSE^{low} CD4⁺ T cells after coculture with BMDCs. (C) Geometric mean fluorescence (gMFI) of (C) anti-FoxP3, (D) anti-RORγT and (E) anti-Tbet antibodies in the population of proliferated CD4⁺ T cells. **p ≤ 0.01, *p ≤ 0.05 determined by one-way ANOVA and Tukey's multiple comparison test.

Administration of DOPG/PLGA hybrid nanoparticles loaded with antigen and vitaminD3 has no effect on atherosclerosis development

Since *in vitro* data showed that vitaminD3 loaded DOPG/PLGA hybrid nanoparticles induced higher FoxP3 expression than DSPG liposomes, we next assessed whether these nanoparticle formulations could affect the development of atherosclerosis. We used LDLR^{-/-} mice with an additional genetic modification to express a ApoB100

tagged with the epitope OVA323, therefore we could use OVA323 as the target antigen for the vaccine formulation.

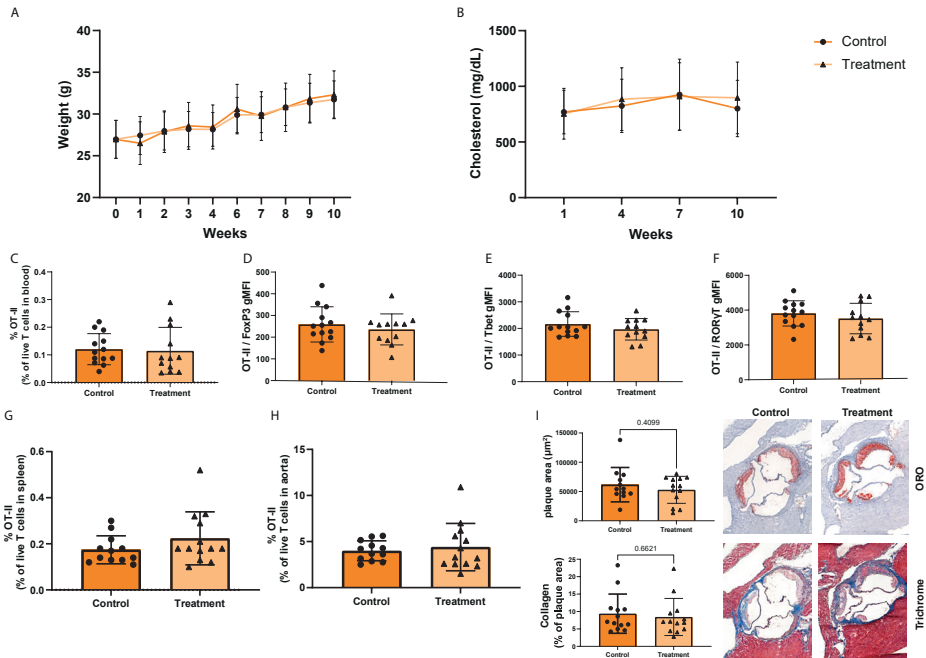


Figure 5. Effect of DOPG/PLGA hybrid nanoparticles on atherosclerosis development. (A) Weight and (B) plasma cholesterol levels of mice during the experiment. (C) Percentage of OT-II CD4⁺ T cells in blood of immunized mice at the end of the experiment. Geometric mean fluorescence intensity (gMFI) of (D) FoxP3, (E) Tbet and (F) RORγT in the OT-II T cell population in blood. Percentage of OT-II CD4⁺ T cells in (G) spleen and (H) aorta of mice at the end of the experiment. (I) Plaque area in μm^2 and collagen content as a percentage of total plaque area, and representative images of Oil-Red-O and trichrome staining of trivalve area slides. Significant differences between control and treatment groups were tested using unpaired two-tailed t test.

We transferred activated OT-II CD4⁺ T cells to the *LDLr^{-/-}* mice and subsequently immunize the mice with either DOPG/PLGA hybrid nanoparticles loaded with OVA323 and vitaminD3 or DOPG/PLGA hybrids loaded with vitaminD3 but no antigen as control (mock vaccination). Average particle size, Pdl and ζ -potential of formulations can be found in Supplementary Figure 1. We performed a total of 3 IV injections of the formulations over the course of 10 weeks. Animals were fed a western-type diet during the 10 weeks of experiment. As expected, weight of the animals steadily increased over the experiment, with no significant differences between the vaccinated and mock vaccinated group (Figure 5A). Furthermore, the concentration of cholesterol in plasma were also not different between the

two groups and remained high throughout the duration of the study (Figure 5B). Surprisingly, we did not observe any difference between the groups in the number or phenotype of OT-II T cells in blood (Figure 5C), spleen (Figure 5G) or aorta (Figure 5H). The Oil-Red-O and trichrome histochemical staining also did not show differences in plaque area or collagen content of the plaques (Figure 5I) between control and treatment groups. These data suggest that the DOPG/PLGA hybrid nanoparticles are not able to induce antigen-specific T cell responses *in vivo* and therefore the treatment has no effect on atherosclerosis development.

Only the DSPG liposomes but not the DOPG/PLGA hybrid nanoparticles are able to induce an antigen-specific T cell response *in vivo*

Due to the lack of *in vivo* response to the immunization with DOPG/PLGA hybrid nanoparticles in the atherosclerosis experiment, we assessed how DOPG/PLGA hybrid nanoparticles compared to the previously reported DSPG liposome formulation and to DOPG liposomes *in vivo*. All formulations were loaded with OVA323 and vitaminD3. Briefly, we transferred 500,000 OT-II OVA-specific CD4⁺ T cells to C57Bl/6 mice and subsequently immunized those mice with the nanoparticle formulations. Empty DOPG/PLGA hybrid nanoparticles or free OVA323 and vitaminD3 were used as controls.

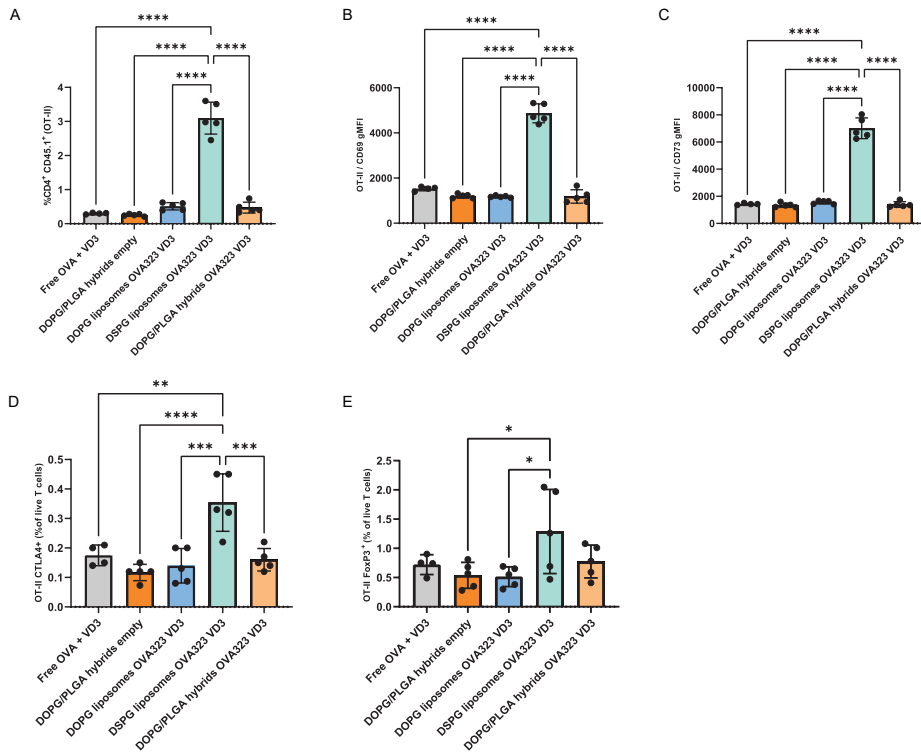


Figure 6. Induction of antigen-specific T cells by nanoparticles in spleen of mice 7 days after intravenous immunization. (A) Percentage of transferred OT-II CD4⁺ T cells in spleens of immunized mice. (B) Geometric mean fluorescence intensity (gMFI) of anti-CD69 antibody in the OT-II CD4⁺ T cell population in spleen. (C) gMFI of anti-CD73 antibody in the OT-II CD4⁺ T cell population in spleen. (D) Percentage of OT-II CD4⁺ T cells expressing CTLA4 and (E) FoxP3 in the live T cell population of the spleen. **** $p \leq 0.0001$, *** $p \leq 0.001$, ** $p \leq 0.01$, * $p \leq 0.05$ determined by one-way ANOVA and Tukey's multiple comparison test.

On day 7 after immunization, we isolated the spleen of the mice and studied the presence of the OVA-specific T cells and their phenotype. In line with the previous *in vivo* experiment, we observed that the DOPG/PLGA hybrid nanoparticles did not induce significantly higher levels of OT-II CD4⁺ T cells compared to the free antigen or the empty DOPG/PLGA hybrid nanoparticle controls, and only the DSPG liposome formulation was able to induce significant antigen-specific T cell proliferation (Figure 6A). Furthermore, only the group immunized with DSPG liposomes showed higher expression of CD69, a marker of recent T cell activation, in the OT-II T cell population (Figure 6B). We also observed an increase in the expression of CD73 (Figure 6C), CTLA4 (Figure 6D) and FoxP3 (Figure 6E), markers

that indicate CD4⁺ Treg activation in the DSPG liposome group. No statistically significant differences between groups were observed in the percentage of OT-II T cells expressing Tbet or ROR γ T (Supplementary Figure 2). These data explain the lack therapeutic efficacy of DOPG/PLGA nanoparticles and underline the importance of *in vivo* testing.

Lipid bilayer composition affects protein corona formation and alters cellular uptake of nanoparticles

Our data shows that although the rigid DOPG/PLGA hybrid particles induce Tregs *in vitro*, their ability to induce them *in vivo* is lost. Interestingly, the same goes for the most fluid particle, the DOPG liposome, whose lipid composition is different to the DSPG liposome but similar to the DOPG/PLGA hybrid particles. We have previously shown that the capacity to induce Tregs of DSPG liposomes depends on the attraction of a protein corona, labelling the particles for uptake via scavenger receptors¹. We hypothesized that potentially the protein corona attracted to DOPG-containing bilayers may differ from DSPG-containing ones, despite both phospholipid classes sharing the same polar headgroup. To determine if these 3 formulations have different capacity to attract proteins to their surface, we first incubated DOPG liposomes, DSPG liposomes and DOPG/PLGA hybrids with mouse serum, FBS or the serum proteins ApoE, ApoB or C1q and determined the effect on particle size (Figure 7A), Pdl (Figure 7B) and ζ -potential (Figure 7C) using DLS. Mouse serum induced a clear increase in particle size of the DSPG liposomes but no significant increase in Pdl, while it only induced a slight increase in particle size in the case of the DOPG/PLGA hybrid nanoparticles but with a bigger effect on Pdl (Figure 7A and 7B).

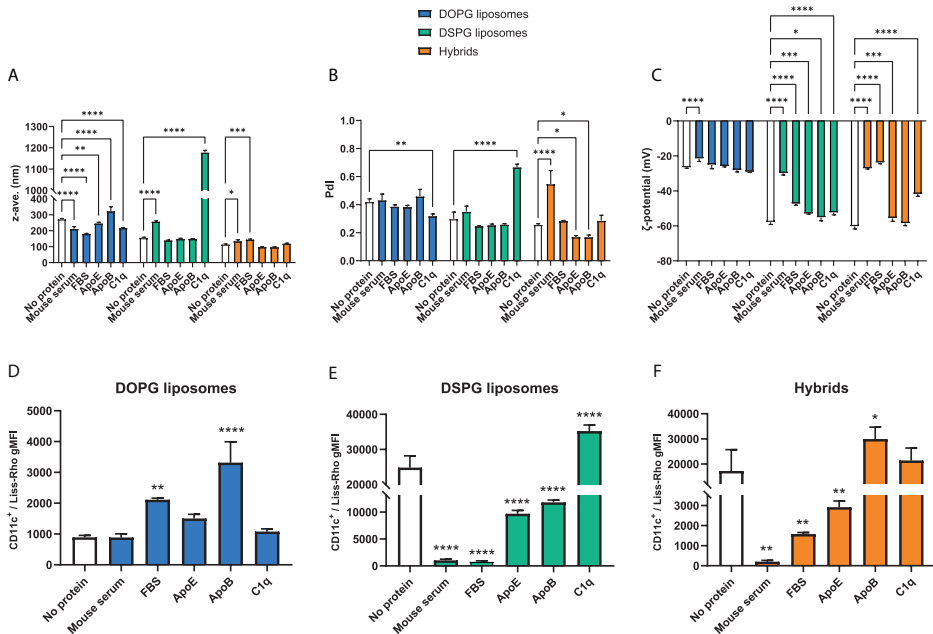


Figure 7. Effect of protein corona on particle characteristics and uptake by BMDCs. Effect of mouse serum, fetal bovine serum (FBS), ApoE, ApoB or C1q on (A) average particle size, (B) polydispersity index and (C) ζ -potential of DOPG liposomes, DSPG liposomes or DOPG/PLGA hybrid nanoparticles. Effect of mouse serum, FBS, ApoE, ApoB or C1q on the uptake of lissamine-rhodamine-labelled (D) DOPG liposomes, (E) DSPG liposomes and (F) DOPG/PLGA hybrid nanoparticles by bone marrow-derived dendritic cells (BMDCs). Geometric mean fluorescent intensity (gMFI) data normalized by subtracting the background fluorescence in nanoparticle-free control. Graphs show mean \pm SD. **** $p \leq 0.0001$, *** $p \leq 0.001$, ** $p \leq 0.01$, * $p \leq 0.05$ compared to no protein condition and determined by (A-C) two-way ANOVA or (D-F) one-way ANOVA followed by Dunnett's multiple comparison test.

This may indicate that DSPG liposomes generate a protein corona when in contact with mouse serum while the DOPG/PLGA hybrid nanoparticles tend to aggregate. There is a clear effect of the Vivaspin purification step in particle size and PDI of DOPG liposomes since the average particle size before Vivaspin is below 200 nm and the PDI is around 0.2 (Supplementary Figure 3), while the PDI is around 0.4 for this formulation after the Vivaspin step (Figure 7B). In the case of particles incubated with FBS, the protein source in cell culture medium used in *in vitro* experiments, there was no significant effect on the particle size and PDI of DSPG liposomes while DOPG/PLGA hybrid nanoparticles increased in average size without affecting PDI. ApoB induced an increase in particle size of DOPG liposomes suggesting the formation of an ApoB protein corona. For DSPG liposomes, only C1q has an impact in particle size (Figure 7A) and PDI (Figure 7B) with a dramatic increase in

both parameters that indicates aggregation of the formulation. In the case of the DOPG/PLGA hybrid nanoparticles the incubation with ApoE, ApoB or C1q did not increase particle size (Figure 7A) or Pdl (Figure 7B). Changes in ζ -potential are also indicative of the adsorption of proteins to the nanoparticle surface. In the case of DOPG liposomes only the incubation with mouse serum led to slightly less negative surface charge (Figure 7C). For DSPG liposomes, all the protein conditions tested led to less negative surface charge, with mouse serum having the biggest effect (Figure 7C). For DOPG/PLGA hybrid nanoparticles, all protein conditions except for ApoB led to less negative ζ -potential with the largest effect caused by mouse serum and FBS (Figure 7C).

After studying the effect of protein corona formation on physicochemical properties of the nanoparticles, we next compared the uptake of nanoparticles with and without the different protein coronas by BMDCs. For DOPG liposomes, the protein corona formed after incubation with FBS or ApoB significantly increased the cell uptake (Figure 7D). In the case of DSPG liposomes, only the presence of C1q in the medium led to an enhance uptake by DCs while the rest of the proteins studied significantly reduced cellular uptake (Figure 7E). For DOPG/PLGA hybrid nanoparticles, only the presence of ApoB in the medium led to a significant increase in uptake by DCs (Figure 7F). Interestingly, the presence of mouse serum in the medium abrogated the uptake of DOPG/PLGA hybrids almost completely (Figure 7F). These data show that the DSPG-containing and the DOPG-containing bilayers have different capacity to attract proteins, and this has consequences for the uptake of nanoparticle by DCs, which is the first step in the initiation of an antigen-specific immune response.

DISCUSSION

Phospholipid composition affects the physicochemical characteristics of lipid-based nanoparticles such as ζ -potential and rigidity but also determines the interaction with biomolecules in the environment, i.e. the protein corona. Here, we studied the capacity of “fluid” anionic liposomes (DOPG liposomes), “rigid” anionic liposomes (DSPG liposomes) and DOPG/PLGA hybrid particles covered with a fluid DOPG phospholipid bilayer to deliver antigens to DCs and induce tolerogenic antigen-specific CD4⁺ T cells both *in vitro* and *in vivo*. The use of DOPG/PLGA hybrid nanoparticles allows us to determine the contribution of nanoparticle rigidity independently from the lipid composition. Although the Young’s module of the hybrid nanoparticles has not been determined experimentally, similar lipid-wrapped PLGA nanoparticles have shown to have a Young’s module of 60 ± 32 MPa, in contrast with DOPC:DOPG liposomes (0.493 ± 0.365 MPa) and DSPC:DSPG:CHOL liposomes (1.498 ± 0.530 MPa)^{6, 17}.

We observed that the exposure of BMDCs to empty DOPG/PLGA hybrid nanoparticles leads to a reduced activation level, measured by the expression of CD86 and CD40, upon pro-inflammatory stimulation with LPS. This effect was also observed in both DOPG and DSPG liposomes when the tolerogenic adjuvant vitaminD3 was included in the formulation. These results are in line with previous reports showing that delivery of vitaminD3 using anionic liposomes is able to induce regulatory or tolerogenic phenotype on DCs⁷. Interestingly, DSPG liposomes without vitaminD3 did not seem to induce this tolerogenic phenotype, although these liposome formulations have previously shown to be able to induce a Treg response in mice¹. The mechanism of action of Treg induction by DSPG liposomes has not been elucidated yet, although our data suggests that it is not through the inhibition of CD86 and CD40 expression. Similarly, a report from Braake & Benne et al. (2021) showed no effect of non-adjuvated DSPG liposomes on the expression of CD86 and CD40, only when the tolerogenic adjuvant retinoic acid was included in the formulation it was able to induce tolerogenic DCs¹⁸.

We also studied the capacity of nanoparticle-primed DCs to induce antigen-specific T cell responses. We observed that all nanoparticle formulations were able to induce CD4⁺ T cell proliferation (Figure 3A and 3B) demonstrating that the antigen was successfully delivered and presented to T cells. We further characterized the phenotype of the proliferating T cells. The DCs primed with DOPG/PLGA hybrid nanoparticles induced the expression of FoxP3, ROR γ T and Tbet on T cells, transcription factors associated to Tregs, Th17 and Th1 cells respectively, compared to liposome-primed DCs. In contrast to previous reports, DCs primed with DSPG liposomes loaded with antigen or with antigen and vitaminD3 did not induce FoxP3 in the proliferating cells population, however these formulations seemed to reduce expression of Tbet compared to free antigen, indicating a less pro-inflammatory phenotype.

In vitro exposure of DCs to nanoparticles does not fully capture the complexity of biological systems and it does not recapitulate the effect of biodistribution or biological barriers to reach the target cells¹⁹. We therefore studied the effect of the nanoparticles *in vivo*. The DSPG liposomes were able to successfully induce an OVA-specific T cell response as it has been reported in previous studies^{1, 18}. These antigen-specific CD4⁺ T cells also showed higher expression of CTLA4, a co-inhibitory molecule that is key for peripheral tolerance²⁰. On the other hand, the DOPG/PLGA hybrid nanoparticles did not induce antigen-specific T cell responses in neither the atherosclerosis nor the adoptive transfer experiments, explaining its inability to reduce atherosclerosis in the LDLR^{-/-} x ApoB-OVA model. In fact, the *in vivo* behaviour of hybrid DOPG/PLGA particles seemed to be very similar to the fluid DOPG liposomes.

Both DOPG liposomes and DOPG/PLGA hybrids share the same lipid bilayer, and it is the main difference between these formulations and DSPG liposomes. We hypothesized that the difference in lipid bilayer composition might lead to differences in the protein corona, previous research has shown that bilayers composed of unsaturated phospholipids can form lipid domains while the presence of cholesterol in the bilayer disrupts these domains, favours a more homogeneous distribution of the different phospholipids in the bilayer and increases binding of proteins to the nanoparticle surface¹⁰. Therefore, the lack of cholesterol and the unsaturated phospholipid composition in both the DOPG liposomes and the DOPG/PLGA hybrids could lead to quantitative and/or qualitative differences in protein corona and explain the lack of *in vivo* effect of these two formulations. We indeed observed that the incubation of DOPG liposomes, DSPG liposomes and DOPG/PLGA hybrids with mouse serum or FBS influenced their physicochemical characteristics (Figure 7A, B and C). Increase in particle size and Pdl as well as partial neutralization of the surface charge are all clear signs of the formation of a protein corona²¹. There was a clear difference in ζ -potential between DOPG liposomes and DOPG/PLGA hybrids although both formulations have the same lipid bilayer composition. This difference could be due to the use of PBS for the formulation of DOPG liposomes while PB was used for the preparation of DOPG/PLGA hybrids. The clear abrogation of the uptake of DOPG/PLGA hybrids by BMDCs in the presence of mouse serum suggests that the protein corona formed *in vivo* hinders the uptake of these particles by APCs, explaining the lack of antigen-specific immune responses in the mouse experiments. When looking at the effect of individual proteins on the uptake, we observed that C1q greatly enhances the uptake of DSPG liposomes. The role of this complement protein on DSPG liposome uptake has been reported before¹. The increased uptake in this condition can also be potentiated by the particle aggregation observed, since nanoparticle aggregation can lead to enhanced uptake by APCs²². On the other hand, for DOPG liposomes, ApoB seems to play a bigger role in mediating the liposome uptake. The same effect can be observed for the DOPG/PLGA hybrids, however there were no signs of ApoB deposition on these particles in the DLS data. A weaker interaction between ApoB and the DOPG/PLGA hybrids could result in the wash-out of the protein during the purification step before DLS explaining the limited impact of ApoB incubation in the physicochemical properties of DOPG/PLGA hybrids. The lack of *in vivo* effect of the DOPG/PLGA hybrid nanoparticles compared to the DSPG liposomes could therefore be explained by the availability of the different proteins mediating the uptake of these different nanoparticles, in the circulation. While C1q is a complement protein that is freely available in circulation²³, ApoB100 is an amphipathic protein that travels in the bloodstream associated with cholesterol and lipids forming LDL and VLDL

particles²⁴. Furthermore, unlike other lipoproteins ApoB is non-exchangeable so it cannot transfer between different lipoprotein particles²⁵, therefore it is not freely available to adsorb to the nanoparticle surface and mediate their cellular uptake. All in all, our data point towards a more prevalent role of the lipid bilayer composition compared to the particle rigidity in the biological effect of nanoparticles, and those differences in the biological effect seem to be mediated by the protein corona.

CONCLUSIONS

Physicochemical properties of liposomes such as negative surface charge and high rigidity have been previously linked to tolerogenic capacity of these formulations. However, liposome rigidity is mostly determined by the phospholipid composition of the bilayer, which can also determine the protein corona of the particle in a biological environment. The data presented here suggests that the phospholipid composition associated with highly rigid liposomes, i.e. saturated phospholipids, and cholesterol, may be more important in determining the *in vivo* effect of liposomes than the particle rigidity itself.

AUTHOR CONTRIBUTIONS

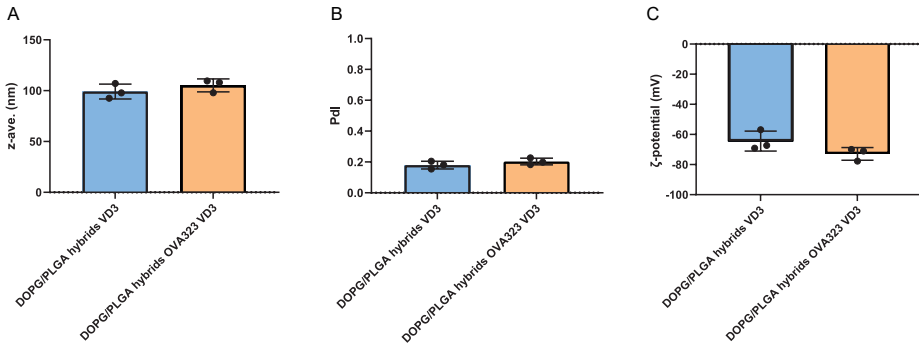
FLV conceptualised the project, designed and carried out experiments, drafted this chapter and prepared the figures. MAN conceptualised the hybrid nanoparticles and developed the formulation method. LHMB and WEH performed part of the experiments. AK, JAB and BS provided valuable input in the experimental design and edited the draft chapter.

REFERENCES

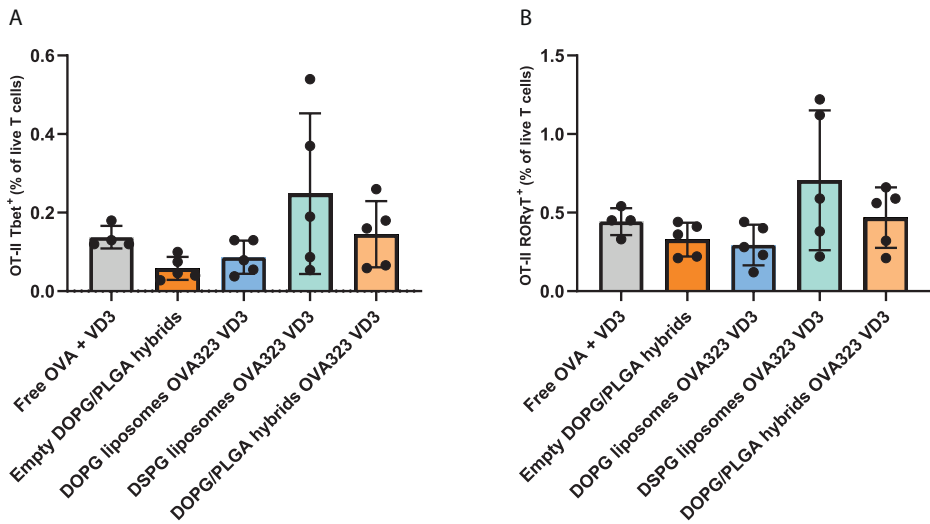
1. Benne N, van Duijn J, Lozano Vigario F, Lebox RJT, van Veelen P, Kuiper J, et al. Anionic 1,2-distearoyl-sn-glycero-3-phosphoglycerol (DSPG) liposomes induce antigen-specific regulatory T cells and prevent atherosclerosis in mice. *J Control Release*. 2018;291:135-46.
2. Pujol-Autonell I, Serracant-Prat A, Cano-Sarabia M, Ampudia RM, Rodriguez-Fernandez S, Sanchez A, et al. Use of autoantigen-loaded phosphatidylserine-liposomes to arrest autoimmunity in type 1 diabetes. *PLoS One*. 2015;10(6):e0127057.
3. Libby P. The changing landscape of atherosclerosis. *Nature*. 2021;592(7855):524-33.
4. Benne N, van Duijn J, Kuiper J, Jiskoot W, Slutter B. Orchestrating immune responses: How size, shape and rigidity affect the immunogenicity of particulate vaccines. *J Control Release*. 2016;234:124-34.
5. Korsholm KS, Hansen J, Karlsen K, Filskov J, Mikkelsen M, Lindenstrom T, et al. Induction of CD8+ T-cell responses against subunit antigens by the novel cationic liposomal CAF09 adjuvant. *Vaccine*. 2014;32(31):3927-35.
6. Benne N, Lebox RJT, Glandrup M, van Duijn J, Lozano Vigario F, Neustrup MA, et al. Atomic force microscopy measurements of anionic liposomes reveal the effect of liposomal rigidity on antigen-specific regulatory T cell responses. *J Control Release*. 2020;318:246-55.
7. Nagy NA, Lozano Vigario F, Sparrius R, van Capel TMM, van Ree R, Tas SW, et al. Liposomes loaded with vitamin D3 induce regulatory circuits in human dendritic cells. *Front Immunol*. 2023;14:1137538.
8. Nakano K, Tozuka Y, Yamamoto H, Kawashima Y, Takeuchi H. A novel method for measuring rigidity of submicron-size liposomes with atomic force microscopy. *Int J Pharm*. 2008;355(1-2):203-9.
9. Beckers D, Urbancic D, Sezgin E. Impact of Nanoscale Hindrances on the Relationship between Lipid Packing and Diffusion in Model Membranes. *J Phys Chem B*. 2020;124(8):1487-94.
10. Nele V, D'Aria F, Campani V, Silvestri T, Biondi M, Giancola C, De Rosa G. Unravelling the role of lipid composition on liposome-protein interactions. *J Liposome Res*. 2023:1-9.
11. Lozano Vigario F, Nagy NA, The MH, Sparrius R, Bouwstra JA, Kros A, et al. The Use of a Staggered Herringbone Micromixer for the Preparation of Rigid Liposomal Formulations Allows Efficient Encapsulation of Antigen and Adjuvant. *J Pharm Sci*. 2022;111(4):1050-7.
12. van Eenige R, Verhave PS, Koemans PJ, Tiebosch I, Rensen PCN, Kooijman S. RandoMice, a novel, user-friendly randomization tool in animal research. *PLoS One*. 2020;15(8):e0237096.
13. Schindelin J, Arganda-Carreras I, Frise E, Kaynig V, Longair M, Pietzsch T, et al. Fiji: an open-source platform for biological-image analysis. *Nat Methods*. 2012;9(7):676-82.
14. Pattipeiluhu R, Crielaard S, Klein-Schiphorst I, Florea BI, Kros A, Campbell F. Unbiased Identification of the Liposome Protein Corona using Photoaffinity-based Chemoproteomics. *ACS Cent Sci*. 2020;6(4):535-45.
15. Viney NJ, Yeang C, Yang X, Xia S, Witztum JL, Tsimikas S. Relationship between "LDL-C", estimated true LDL-C, apolipoprotein B-100, and PCSK9 levels following lipoprotein(a) lowering with an antisense oligonucleotide. *J Clin Lipidol*. 2018;12(3):702-10.

16. Domogalla MP, Rostan PV, Raker VK, Steinbrink K. Tolerance through Education: How Tolerogenic Dendritic Cells Shape Immunity. *Front Immunol.* 2017;8:1764.
17. Eshaghi B, Alsharif N, An X, Akiyama H, Brown KA, Gummuluru S, Reinhard BM. Stiffness of HIV-1 Mimicking Polymer Nanoparticles Modulates Ganglioside-Mediated Cellular Uptake and Trafficking. *Adv Sci (Weinh).* 2020;7(18):2000649.
18. Ter Braake D, Benne N, Lau CYJ, Mastrobattista E, Broere F. Retinoic Acid-Containing Liposomes for the Induction of Antigen-Specific Regulatory T Cells as a Treatment for Autoimmune Diseases. *Pharmaceutics.* 2021;13(11).
19. Ishida T, Harashima H, Kiwada H. Interactions of liposomes with cells in vitro and in vivo: opsonins and receptors. *Curr Drug Metab.* 2001;2(4):397-409.
20. Wing K, Onishi Y, Prieto-Martin P, Yamaguchi T, Miyara M, Fehervari Z, et al. CTLA-4 control over Foxp3+ regulatory T cell function. *Science.* 2008;322(5899):271-5.
21. Xiao Q, Zoulikha M, Qiu M, Teng C, Lin C, Li X, et al. The effects of protein corona on in vivo fate of nanocarriers. *Adv Drug Deliv Rev.* 2022;186:114356.
22. Liu X, Chen Y, Li H, Huang N, Jin Q, Ren K, Ji J. Enhanced retention and cellular uptake of nanoparticles in tumors by controlling their aggregation behavior. *ACS Nano.* 2013;7(7):6244-57.
23. van de Bovenkamp FS, Dijkstra DJ, van Kooten C, Gelderman KA, Trouw LA. Circulating C1q levels in health and disease, more than just a biomarker. *Mol Immunol.* 2021;140:206-16.
24. Segrest JP, Jones MK, De Loof H, Dashti N. Structure of apolipoprotein B-100 in low density lipoproteins. *J Lipid Res.* 2001;42(9):1346-67.
25. Gordon SM, Pourmoussa M, Sampson M, Sviridov D, Islam R, Perrin BS, Jr., et al. Identification of a novel lipid binding motif in apolipoprotein B by the analysis of hydrophobic cluster domains. *Biochim Biophys Acta Biomembr.* 2017;1859(2):135-45.

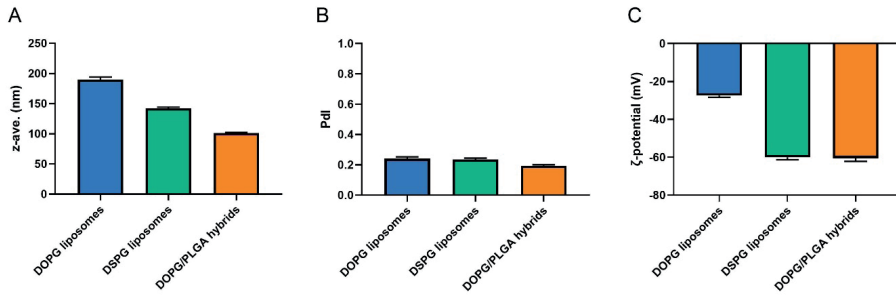
SUPPLEMENTARY DATA



Supplementary Figure 1. Physicochemical characteristics of formulations used in atherosclerosis experiment. (A) Average hydrodynamic diameter of the nanoparticles (Z-average) in nm, (B) Polydispersity Index and (C) ζ -potential in mV of DOPG/PLGA hybrids nanoparticles loaded with vitaminD3 only and with vitaminD3 and OVA323. Data shown is mean \pm SD.



Supplementary Figure 2. Th1 and Th17 OT-II T cells in spleen of mice 7 days after immunization. (A) Percentage of OT-II T cells expressing the Th1 transcription factor Tbet and (B) the Th17 transcription factor ROR γ T in the live T cell population of the spleen. Statistically significant differences between groups tested by one-way ANOVA and Tukey's multiple comparison test.



Supplementary Figure 3. Physicochemical characteristics of nanoparticle formulations before the Vivaspin centrifugation step in the protein corona study. (A) Average particle size, (B) Polydispersity Index and (C) ζ -potential of the formulations incubated in buffer at 37°C for 1h. Data shown is mean \pm SD.